PHYSICAL REVIEW B VOLUME 39, NUMBER 15 15 MAY 1989-II

Photoemission studies of interface chemistry and Schottky barriers for ZnSe(100) with Ti, Co, Cu, Pd, Ag, Au, Ce, and Al

M. Vos, F. Xu, Steven G. Anderson, and J. H. Weaver
Department of Chemical Engineering and Materials Science, University of Minnesota, Minneapolis, Minnesota 55455

H. Cheng
3M Company, 3M Center, St. Paul, Minnesota 55144
(Received 8 September 1988)

Photoemission has been used to examine the formation of metal overlayers on sputter-annealed ZnSe(100)-$c(2\times2)$ surfaces for transition metals (Ti,Co), noble and near-noble metals (Cu,Ag,Au,Pd), a lanthanide (Ce), and a simple metal (Al). Analysis of Zn $3d$ core-level emission reflects metal-substrate interaction as well as substrate band bending as a function of metal coverage. Large differences in chemical behavior have been found. In particular, Ag and Au adatoms induce negligible Zn $3d$ core-level broadening, which is consistent with no substrate disruption. For the other metals, a second Zn $3d$ component reflects substrate disruption, and two reaction-induced components develop for Ti and Ce. The development of the Schottky barrier is compared with work-function variations. Very different Schottky-barrier heights have been found, ranging from 0.5 eV for Ce to 1.5 eV for Au and Pd. Neither the defect model nor the metal-induced gap-states model is able to describe all the experimental Schottky-barrier data. We do find a general correlation between the barrier height and the metal work function.

INTRODUCTION

Metal semiconductor interfaces have been studied extensively with a variety of surface and bulk techniques.[1] Although a wealth of experimental data is now available, many of the basic questions remain, including the mechanism of substrate disruption and the correlation of the state of the interface and the Schottky-barrier height (SBH). Recent photoemission studies that have examined the formation of interfaces at low temperature have raised questions about overlayer nucleation, reaction, and barrier formation.[2]

The most extensively studied semiconductor interfaces have involved the III-V compounds, particularly GaAs and InP. Much less has been done with the II-VI compound semiconductors, and a relatively small number of photoemission studies have been reported.[3] The purpose of this paper is to examine the results of a systematic study of metal-ZnSe(100) interface formation, where the metals chosen are representative of the transition metals (Ti,Co), the noble and near-noble metals (Cu,Ag,Au,Pd), a rare earth (Ce), and a simple metal (Al). In so doing, we have varied the electronegativity and reactivity of the adatoms to identify trends of interface formation.

Metal-ZnSe interfaces are interesting for several reasons. First, the heat of formation of ZnSe (-163 kJ/mol) is nearly twice as large as for CdTe (-92 kJ/mol) or the covalent semiconductors GaAs and InP (-88 and -88.7 kJ/mol, respectively).[4] Comparisons with these materials then provide insight concerning the importance of substrate bond strength for reaction and substrate disruption. Second, the ZnSe bond has a relatively large ionic character. In particular, it was noted several years ago that Schottky-barrier formation would be different for the ionic materials compared to the covalent semiconductors.[5,6] For many of the more covalent semiconductors, the Schottky-barrier heights varied relatively little for different metals,[7,8] and models based on the intrinsic properties of the semiconductor were developed.[9] For the ionic semiconductors, however, the SBH's were found to depend strongly on the metal overlayer and can be described rather well by the Schottky model, where the SBH reflects the difference of metal and semiconductor electron affinity. One of the goals of this study was then to correlate SBH formation to reactivity at the interface and the properties of the metal. The relatively large band gap of ZnSe (2.7 eV) makes it possible to observe SBH changes which are large compared to experimental errors. As we will show, there is no simple relation between interface reactivity and Schottky-barrier development. However, a general correlation between the final SBH and the metal work function is observed.

In the following, we describe the experimental procedures, present the experimental results, and focus on the chemistry of metal-ZnSe interfaces. Thereafter, we will examine issues related to the SBH. Studies of the effects of metal interlayers are published elsewhere.[10,11]

EXPERIMENTAL DETAILS

Undoped, n-type ZnSe(100) samples were grown on GaAs(100) substrates using molecular-beam epitaxy (MBE).[12] Clean surfaces were subsequently prepared in the measurement chamber by sputtering with 600-eV Ar^+ ions, followed by annealing at 400 °C for 20 min. The surface structure, determined with low-energy elec-

 ©1989 The American Physical Society

tron diffraction (LEED), was found to be $c(2\times2)$ reconstructed, which corresponds to a Zn-terminated surface.[12] Auger-electron spectroscopy was used to confirm the cleanliness of the sample. Ultraviolet photoemission spectra ($h\nu=21.2$ and 40.8 eV) were taken using a cylindrical-mirror analyzer operating at a pass energy of 10 eV; this corresponds to an overall experimental resolution of ~0.15 eV.

Since the band gap of ZnSe is 2.7 eV and the sample was undoped, it was possible that sample charging or surface photovoltaic effects might induce artificial shifts of the energy-distribution curves (EDC's). Since no shifts were observed in the Zn 3d binding energy or the valence bands due to changes in photon flux and almost no changes (<0.04 eV) were caused by illumination of the sample with a high-intensity incandescent lamp, we conclude that changes in the core-level energy position of the substrate during interface formation were induced only by the metal adatoms.

Adatoms of the different metals were evaporated from thoroughly degassed W baskets, W boats, or Ta boats. The amount of metal deposited was monitored with an Inficon crystal oscillator situated close to the sample. The evaporation rate was typically ~0.5 Å/min and the source to sample distance was ~30 cm. The base pressure was 8×10^{-11} Torr (during He lamp operation the pressure rose to 1×10^{-9} Torr). The incremental change during evaporation was $(3-4)\times10^{-10}$ Torr.

The Zn 3d core-level EDC's were analyzed using a nonlinear least-squares minimization routine that has been described in detail elsewhere.[13] Spectral features were fit by simultaneously varying a cubic polynomial background function and physically realistic core-level line shapes to achieve the best fit. The width of the shallow Zn 3d core level studied here reflects a combination of spin-orbit splitting and dispersion in k space, together with lifetime effects and experimental resolution. Substrate core-level features could be fit with a Lorentzian of width 0.15 eV, a Gaussian of width 0.67 eV, and a spin-orbit splitting of 0.36 eV. This spin-orbit splitting was constrained to be close to the experimental value of 0.34 eV measured for free Zn atoms in metallic, rather than ionic, configurations.[14] The Gaussian width of reacted or dissociated Zn components varied with coverage due to the changing chemical environment of the Zn atoms in the overlayer, as we will discuss. The Lorentzian width, reflecting lifetime broadening of the core level, was kept constant for all components. In certain cases the Gaussian width was narrow enough to observe the Zn 3d spin-orbit splitting.

For Au, Co, and Ti interfaces, x-ray photoemission (XPS) studies were also done in a different experimental chamber. The sample preparation was identical. Monochromatized Al $K\alpha$ radiation and a hemispherical analyzer (Surface Science Instruments 100-03) allowed for high-energy resolution (0.7 eV full width at half maximum for the Au $4f_{7/2}$ photoemission peak). In this way, it was possible to obtain complementary information concerning the Se-atom distribution.

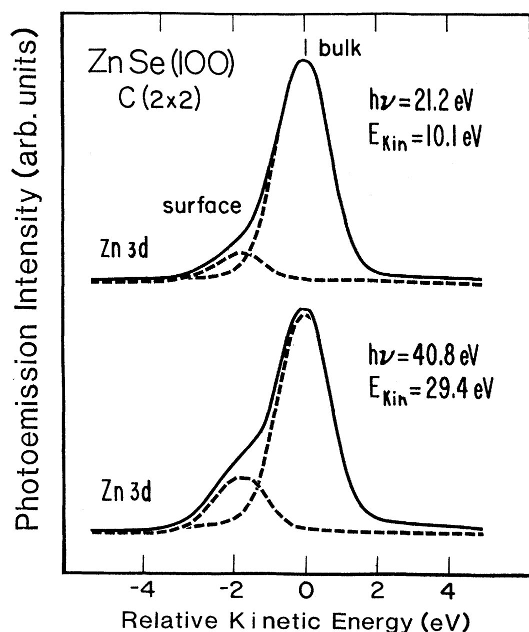

FIG. 1. Zn 3d shallow core-level photoemission spectra taken for $h\nu=21.2$ and 40.8 eV. Both are background subtracted and normalized. The zero in kinetic energy corresponds to 10.1 or 29.4 eV for two spectra, and the spectra are aligned to the bulk Zn emission. The shoulder at 0.9 eV lower kinetic energy reflects a surface core-level shift.

EXPERIMENTAL RESULTS

The ZnSe(100) surface

After sputtering and annealing of the ZnSe(100) surface, the Fermi level E_F was found to be 2.05 eV with a spread between different samples of ±0.1 eV above the valence-band maximum. The background-subtracted Zn 3d spectra of these clean surfaces taken with $h\nu=21.2$ and 40.8 eV are shown in Fig. 1. A clear surface-shifted component can be seen at a 0.9-eV higher-binding energy relative to the main peak, and the intensity of this component is greater in the more surface-sensitive measurements at 40.8 eV.[15,16] Indeed, in Ref. 16 we have compared the intensity ratio of the bulk component and the surface component for photon energies of 21.2–1486.6 eV. Those results indicated that the surface layer corresponds to approximately one-half of a Zn layer, and this is consistent with the $c(2\times2)$ LEED pattern. It is also consistent with theoretical considerations based on electrostatic arguments that a polar surface cannot be terminated by a complete layer of either cations or anions.[17]

Interface chemistry

To characterize the evolving metal-ZnSe interface, we followed the Zn 3d core-level EDC's as a function of metal coverage. Our results show that the interfaces can be classified in three groups, namely nondisruptive (Ag and Au), disruptive (Co, Cu, Pd, and possibly Al), and disruptive and reactive (Ti and Ce). We discuss each of these in

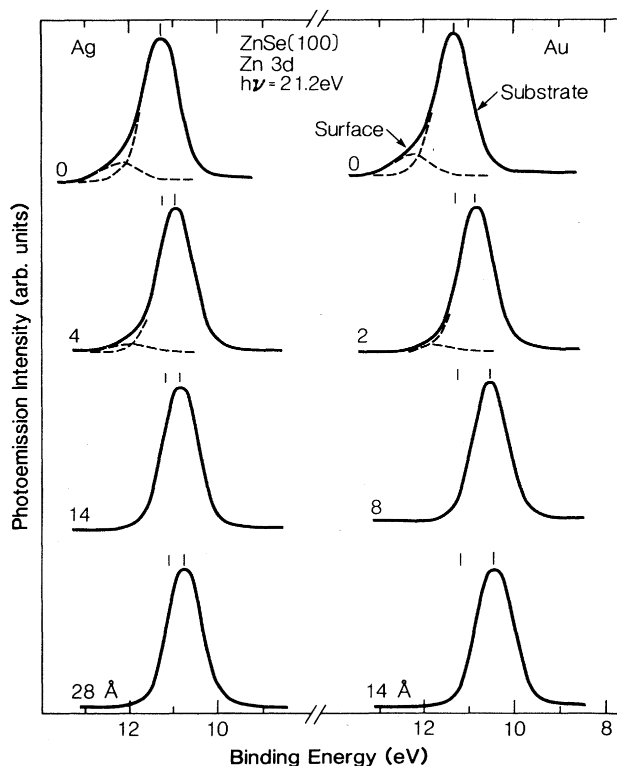

FIG. 2. Background-subtracted, normalized Zn $3d$ spectra for ZnSe(100) with tic marks that identify the maxima for the clean surface and for the interface during Ag and Au deposition. The amount of material deposited is given alongside each spectrum. The surface component disappears gradually, and there is a gradual shift to lower binding energy, but no broadening, indicating the absence of adatom-induced chemical reaction with the substrate.

the following. Before doing so, we note that for Co and Au overlayers, where the lattice match between ZnSe and the metal suggests possible epitaxy, the LEED patterns deteriorated quickly with metal coverage and disappeared completely after ~ 3 Å. We conclude that epitaxial growth was minimal for room-temperature deposition.

In Fig. 2 we show representative Zn $3d$ spectra for deposition of Ag and Au on ZnSe(100). These spectra have been background subtracted and normalized to emphasize line-shape changes; it should be clear that the total Zn $3d$ integrated emission diminishes with metal deposition as the overlayer attenuates substrate photoelectrons. As can be seen from Fig. 2, the Zn $3d$ surface component quickly disappears as the surface layer is modified. Figure 2 also shows a shift to lower binding energy of the substrate Zn $3d$ peak during interface formation. These shifts are a consequence of band bending and will be discussed in the next section. It is important to note that there is no evidence of significant Zn $3d$ broadening (changes less than 0.05 eV in full width at half maximum) or the appearance of the Zn components that could be associated with disruption or reaction during Au or Ag overlayer growth. XPS results for Au also showed no peak broadening in either the Zn $2p$ or Se $3p$ core-level emission. The absence of a second peak in the Zn spectra after Au deposition was also reported by Brillson *et al.*[3] We conclude that there was no disruption of the surface and no dissolution of Zn or Se in the overlayer. For Au, the rapid extinction of substrate emission indicates that the Au/ZnSe interface is an example of the seldom-encountered, nondisruptive, layer-by-layer growth mode.[10] In contrast, while the deposition of Ag does not produce disruption, the slow extinction of the substrate indicates an island-growth mode starting at low coverage, as is typical of Ag growth on semiconductors.[18]

A striking difference between ZnSe and many other semiconductors is that Au atom deposition does not induce disruption for ZnSe while it does for group-IV and -III-V cases studied to date, namely Ge, Si, GaAs, InP, and InSb (Ref. 19 and citations therein). Au adatom-induced disruption has also been observed for CdTe.[3] Its absence for Au/ZnSe may be due to the large cohesive energy of ZnSe.

In Fig. 3 we show representative Zn $3d$ core-level EDC's for the second group composed of Al, Co, Cu, and Pd. For these systems, a new feature appears at lower binding energy, and this adatom-induced component is a clear sign of substrate disruption. We associate it with Zn atoms released from the ZnSe surface and dissolved in the growing overlayer. The relative intensity of this dissolved component grows slowly with deposition, dominating the spectra for Co and Pd coverages greater than ~ 10 Å. Quantitative intensity analysis shows the rapid attenuation of the substrate component for Co, Cu, and Pd, suggesting layer-by-layer growth. It also shows that the rate of attenuation of the dissolved component is much slower, consistent with the redistribution of dissolved atoms in the overlayer, as discussed for many other metal-semiconductor systems.[20] For Co, Cu, and especially Pd the dissolved component is clearly narrower than the substrate $3d$ core level (Gaussian width 0.67 eV for the substrate and 0.30 eV for the disrupted Zn component for Pd deposition). This Zn $3d$ narrowing is not unexpected. In ZnSe, the Zn $3d$ electronic states broaden into bands and exhibit k-space dispersion. Likewise, for Zn metal the measured Zn $3d$ band dispersion is ~ 0.2 eV and the full bandwidth of ~ 1 eV compares well with calculations.[21] In contrast, the $3d$ electrons for the disrupted Zn atoms in solution have little overlap with states derived from the host, and the width approaches that for free Zn atoms.

The results for Al appear to be more complicated because there is an Al-induced component, which is relatively small, and strong substrate Zn $3d$ emission persists, as shown in Fig. 3. Examination of the literature shows that this behavior is quite typical of Al overlayers on semiconductors.[22] In particular, the modification that is seen at low coverage is curtailed, and islands of Al nucleate and grow. The Al/ZnSe results show that substrate modification is characterized by a variety of inequivalent Zn chemical configurations, and there is no line-shape sharpening analogous to that observed for Pd, Cu, or Co. Although fitting of the Zn $3d$ spectra after Al deposition is possible with three components, no clear-cut

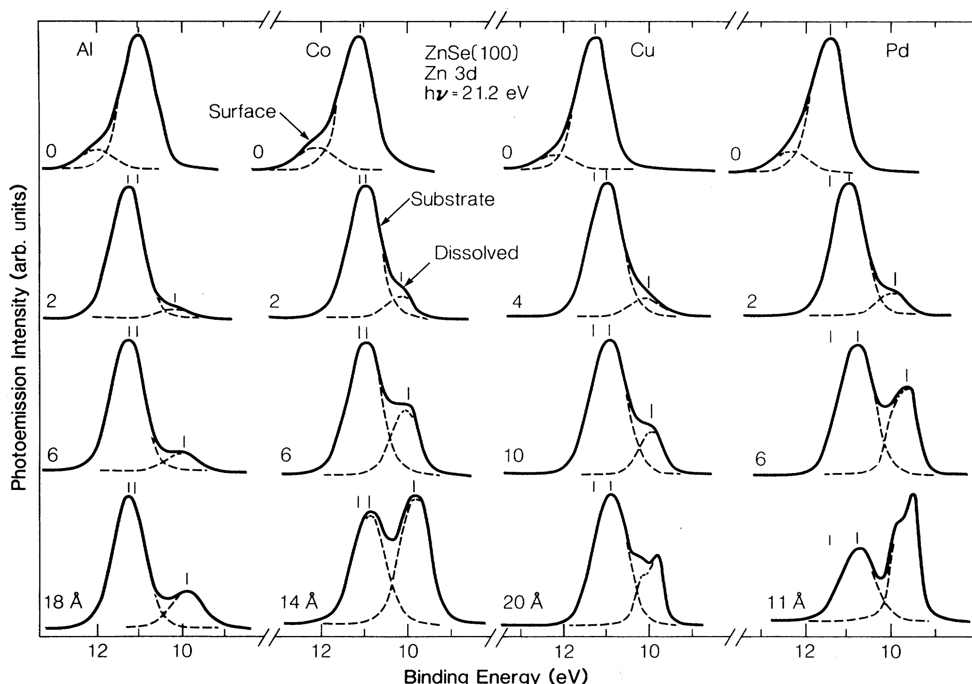

FIG. 3. Zn 3*d* emission as a function of deposition for Al, Co, Cu, and Pd. Surface disruption is reflected by the appearance of a low-binding-energy component which is related to Zn atoms dissolved in the surface and near-surface region of the metal overlayer. For Co, Cu, and Pd, the adatom-induced component is sharper than the substrate component, and for Pd, the Zn 3*d* spin-orbit splitting is observable, as discussed in the text.

and unique decomposition is evident.

The metals Ti and Ce represent a third group, as far as interactions with ZnSe surfaces are concerned, and the results of Fig. 4 show complex behavior. During the early stages of formation, the surface component is lost and structures appear on the low-binding-energy side of the substrate Zn 3*d* peak. The line shape of these new features is complex, and two adatom-induced components are needed to obtain reasonable fits, as shown in Fig. 4. The first, which appears at ~ 0.8 eV lower binding energy, reaches a maximum relative intensity at ~ 6-Å deposition. With progressive metal deposition, it is then attenuated and the rate of attenuation equals that of the substrate component. We associate it with Zn atoms disrupted from ZnSe and reacted or trapped near the interface. Hence, it is identified as "reacted" in Fig. 4. The second component, which is shifted ~ 1.6 eV relative to the substrate signal, dominates the spectra at higher coverage and can be associated with Zn atoms dissolved in the metal overlayer, possibly segregated in the near-surface region. For Ce/ZnSe, the dissolved Zn atoms can be easily observed for coverages in excess of 30 Å, a clear indication of segregation. At this coverage, the substrate and reacted peak can no longer be distinguished above background.

The persistence of Zn 3*d* emission for coverages beyond which the buried interface should no longer be visible indicates Zn surface segregation (coverages greater than ~ 3 times the photoelectron mean free path[15,16]). A

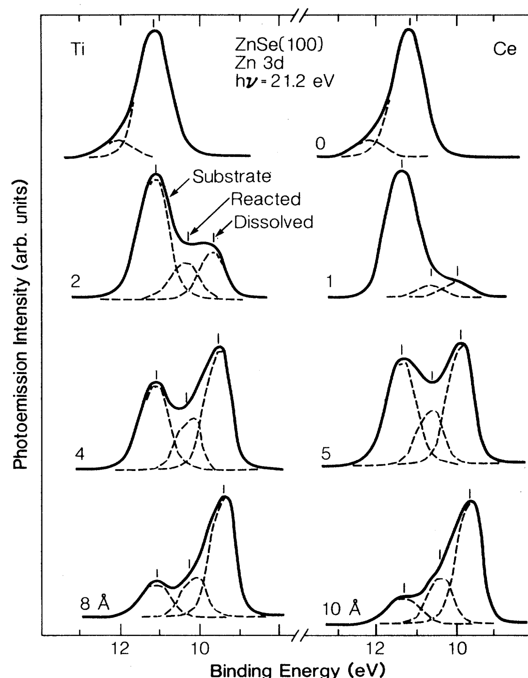

FIG. 4. Zn 3*d* emission as a function of deposition for the reactive metals Ti and Ce. The two adatom-induced components correspond to Zn atoms near the interface (labeled reacted) and dissolved (or segregated) in the metal overlayer.

recently formulated model that describes surface segregation[20] predicts Zn segregation for almost all metal overlayers. In that model, segregation is energetically favored if the dissolved species has a lower cohesive energy (or related to this, a lower melting point) than the overlayer material. Further, segregation is more effective if the dissolved atoms are larger than the overlayer atoms because of strain energies. In this sense, Zn is particularly interesting because its low cohesive energy (-130 kJ/mol) favors segregation, but it is relatively small. From the data, the clearest evidence for segregation is found for Ce overlayers and, to a lesser extent, for Pd overlayer growth on ZnSe. XPS results with greater probe depths[16] show that Zn does not exhibit significant segregation for Ti (Ref. 16) or Co (Ref. 10). It is rather disappointing to note that segregation occurs for Ce but not for Co, although size, melting point, and cohesive energy are all much more favorable for segregation for Co than for Ce. Hence, Co does not seem to fit well with the model predictions.[20] This may be simply a matter of degree since Co induces less disruption than Ce, and Ce forms strong Ce—Se bonds. (Similar results for Co/GaAs showed minimal Ga segregation, despite predictions to the contrary.) Finally, in XPS experiments we found that Se segregated to the surface of both Co and Ti, and this was also reflected in the valence bands as structure ~ 4.5 eV below E_F.

The binding energies of Zn dissolved or segregated in the metals studied are given in Table I. This energy is compared with the binding energy of Zn dissolved in these metals in dilute limit as calculated with the Miedema model[23] using a Born-Haber cycle as described by Johansson *et al.*[24] These calculated energy shifts are relative to pure Zn metal where the Zn 3*d* binding energy for Zn metal is 10.1 eV.[25] The overall agreement, which is reasonable, is consistent with the finding that the component at lowest binding energy corresponds to Zn in the surface and near-surface region.

Schottky-barrier formation

One of the motivations behind metal-semiconductor interface studies is the interest in the electrical properties, i.e., the Schottky barrier.[26] Schottky[27] described the alignment of the Fermi level across the junction in terms of a metal-induced depletion layer in the semiconductor which causes band bending. The barrier height then equals the difference between the metal work function ϕ_M and the semiconductor electron affinity χ, namely,

$$\phi_{SB} = \phi_M - \chi \; . \qquad (1)$$

Bardeen[28] proposed that an accumulation of charge near the interface would produce a dipole which causes the Fermi levels to align. Charge near the interface can be attributed to defect states[29] or to metal-induced-gap states (MIGS).[30] In the defect model, intrinsic semiconductor defects that are created during metal deposition at low coverage and the Fermi-level-pinning position is independent of the metal overlayer. MIGS are the tails of the overlayer wave functions that extend into the semiconductor. The effective valence-band or conduction-band character of these states is determined by the charge-neutrality point. States below the charge-neutrality point have mainly valence-band character and represent positive charge at the surface, if they are not occupied. States above the charge-neutrality point have mainly conduction-band character and tend to represent negative charge, if they are occupied. MIGS tend to pin the Fermi level near the charge-neutrality point. For ZnSe, Tersoff has calculated that the charge neutrality point lies 1.7 eV above the valence-band maximum, but cautions that the charge-decay length in the semiconductor is very short.[30] Cardona and Christensen discussed heterojunction-band offsets and calculated a dielectric midpoint energy of 1.44 eV for ZnSe and showed that this energy is closely related to the charge-neutrality point.[31]

TABLE I. Summary of results for metal-ZnSe(100) interfaces. The second and third columns give the measured and calculated binding energies relative to E_F for Zn atoms dissolved in the metal overlayer. The calculated values are obtained from Ref. 23. The fourth column gives the measured Schottky-barrier heights determined for the highest metal coverage studied. The fifth column gives the metal work function compiled in Ref. 32, and the sixth column lists the barrier height predicted by the Schottky formula using the electron affinity of the $c(2\times2)$ ZnSe(100) surface, 3.51 eV. All energies are given in eV.

Metal	Experimental binding energy for dissolved Zn	Calculated binding energy for dissolved Zn	ϕ_{SB}	ϕ_M	$\phi_{SB}=\phi_M-\chi$
Al	9.8	10.1	0.58	4.20	0.70
Ti	9.3	9.4	0.85	4.33	0.83
Co	9.6	9.6	1.00	4.63	1.50
Cu	9.7	9.7	1.10	4.65	1.15
Pd	9.1	9.4	1.48	5.12	1.62
Ag			1.06	4.26	0.76
Ce	9.6	9.5	0.50	2.9	-0.60
Au			1.45	5.1	1.60

To determine the Schottky-barrier height for these metal-ZnSe interfaces, we measured the position of the valence-band maximum (VBM) relative to the Fermi level (determined at high-metal coverage, estimated accuracy ± 0.03 eV) of the spectrometer by extrapolating the valence-band edge to zero intensity (estimated accuracy ± 0.05 eV). Changes in band bending were then determined from the position of the Zn $3d$ substrate emission as a function of metal coverage. This energy was determined by fitting the background-substrated spectra with the convolution of a Lorentzian and a Gaussian, as noted above (statistical error less than 0.03 eV for nondisruptive metals, 0.05 for reactive metals at high coverage). The SBH was then found by referring E_F to the conduction-band minimum (CBM), using the band-gap value for ZnSe of 2.70 eV. The accuracy of this procedure, together with the reproducibility from one set of measurements to the next for a given metal on ZnSe (typically 0.05 eV), leads to a very conservative estimate of the overall error of ± 0.1 eV.

To determine the electron affinity and surface-work-function changes during interface formation, we biased our sample and measured the secondary-photoelectron-onset energy or vacuum level, E_{vac}. The electron affinity χ is then given by

$$\chi = h\nu - (E_{\text{VBM}} - E_{\text{vac}}) - E_g \ , \quad (2)$$

and the work function by

$$\phi = h\nu - (E_F - E_{\text{vac}}) \ . \quad (3)$$

The measured electron affinity for sputter-annealed

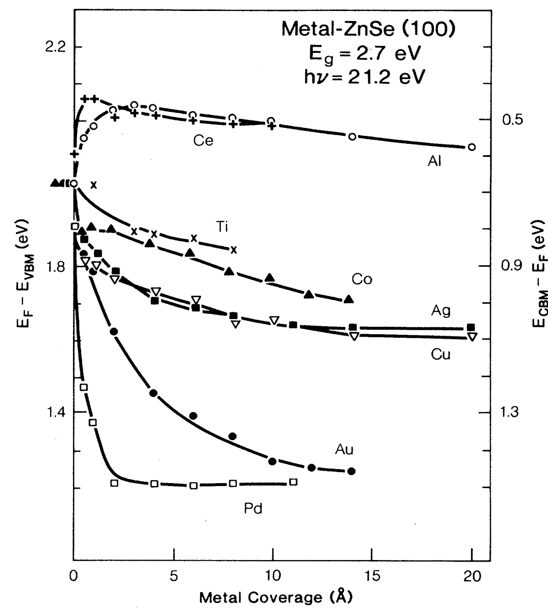

FIG. 5. The evolution of the Fermi-level position in ZnSe as a function of metal deposition. For these systems, the movement of E_F is gradual, and the final position is highly dependent on the metal overlayer. In many cases, the Schottky barrier is not fully established at the highest metal coverage studied, and the barrier height expected for a thick metal layer is likely to be larger than given in the figure or Table I.

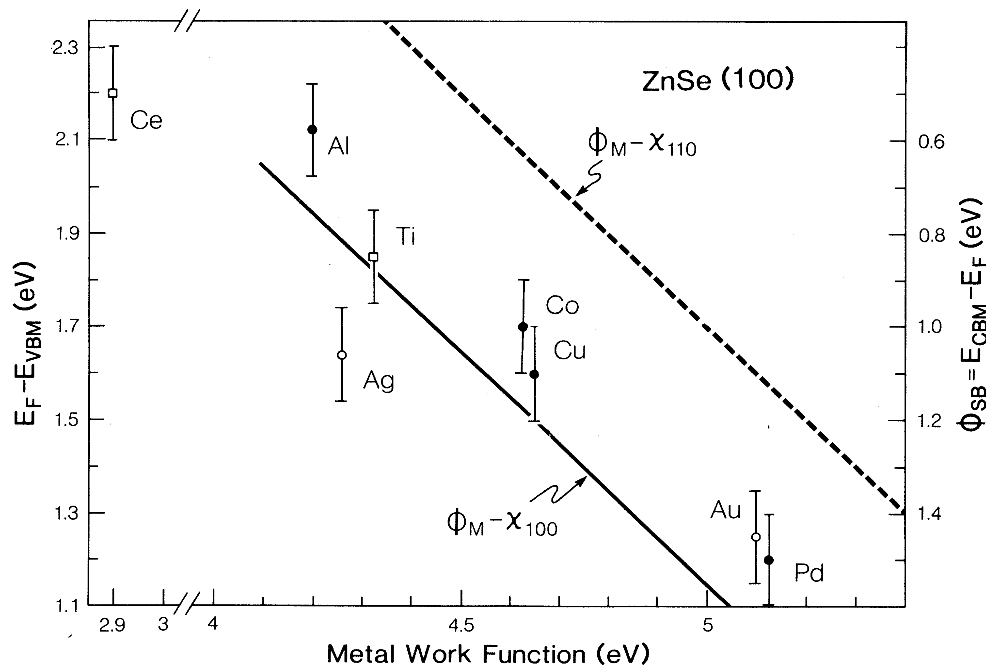

FIG. 6. Schottky-barrier height plotted against overlayer work function (from Ref. 32). The solid line corresponds to the predicted values according to Eq. (1) based on the measured electron affinity of the $c(2\times 2)$ ZnSe(100) surface. The dashed line is based on the electron affinity of cleaved ZnSe(110). Open symbols denote nondisruptive metals, solid circles denote disruptive metals, and squares denote metals that disrupt and react.

ZnSe(100)-$c(2\times2)$ was 3.51 ± 0.1 eV. This is smaller than for a cleaved, nonpolar (110) surface, namely, 4.06 ± 0.1 eV as measured for a cleaved, nonpolar (110) surface. The difference is a result of the dipole caused by the Zn layer that terminates the ZnSe(100)-$c(2\times2)$ surface. Metal deposition, especially when it disrupts the substrate, changes this atomic arrangement and, hence, alters the effective electron affinity. As a result, SB formation for polar (100) surfaces is even more complicated than for simple nonpolar surfaces.

In Fig. 5 we summarize Schottky-barrier-height development for the metal-ZnSe(100) interfaces. Table I lists values obtained at high coverage. The lowest SBH is 0.5 eV for Ce and the highest is 1.45 eV for Pd, giving a spread of ~1 eV. In most cases, the process of band bending is gradual, with completion only after deposition of at least 10 Å of metal but with marked changes at low coverage. For Ce and Al, the SBH development is not monotonic since E_F first moves sharply toward the CBM but then shifts gradually back. From the results of Fig. 5, it is clear that two basic considerations behind the defect model do not apply for ZnSe: that band bending is completed with the deposition of a monolayer and that the final position is independent of the metal. Likewise, the MIGS model does not predict the pinning position accurately. The pinning position varies widely from the calculated values of the charge neutrality point (1.7 or 1.44 eV above the VBM).

Although the defect and MIGS models do not describe the wide range of SBH's for these systems, the use of Eq. (1) allows an approximate correlation of the SBH and the metal work function. Table I summarizes the SBH's predicted by Eq. (1) based on the measured electron affinity of 3.51 eV for ZnSe(100)-$c(2\times2)$ and metal work functions from a compilation by Michaelson for polycrystalline materials.[32] We used the polycrystalline values because we have no indication of epitaxy for any of the metal overlayers. However preferential orientation of the crystallites in the metal film is possible, and this might introduce deviations of the work function of these metal films from the polycrystalline case. The results of Fig. 6 show that there is a general correlation between the SBH and the metal work function, as predicted by Eq. (1), but it is also clear that Eq. (1) cannot accurately predict the magnitude of the SBH.

As a caution, we note that the electron affinity is lower for the Zn-terminated (100) polar surface than for the nonpolar (110) surface. As discussed above, it is likely that the effective affinity, which is related to a specific surface geometry, changes after deposition of a reactive metal. In Fig. 6, we therefore show the predictions of Eq. (1) using the electron affinity for the (100) surface and that for a cleaved (110) surface (dashed line). It is encouraging that most experimental barrier heights (with a clear exception of Ce) lie between these lines.

It is interesting to compare these ZnSe results with the SBH as found in the much studied GaAs case. McLean and Williams[33] recently presented work function and SBH correlations for GaAs that are analogous to those of Fig. 6. Their results and ours show a general correlation between the overlayer work function and the SBH, but with a large scatter around any straight line. However, the SBH dependence on the overlayer work function for ZnSe (total SBH variation 0.98 eV) is much stronger than measured for cleaved GaAs(110) (total variation 0.25 eV) surfaces, as expected for this more ionic semiconductor.[5] Viturro *et al.*[34] recently studied SBH evolution for metals deposited onto MBE-grown GaAs(100). They found a larger SBH spread than for cleaved GaAs(110) (total variation 0.7 eV). They attributed this to a lower defect density in MBE-grown samples relative to bulk crystals. For our sputter-annealed ZnSe(100) surfaces, it is unlikely that there is a very low density of surface defects. Thus the difference in Schottky-barrier formation observed relative to the one usually observed for cleaved GaAs crystals may be due to the different growth technique, or a consequence of the polar (100) surface, rather than a difference between intrinsic GaAs and ZnSe properties.

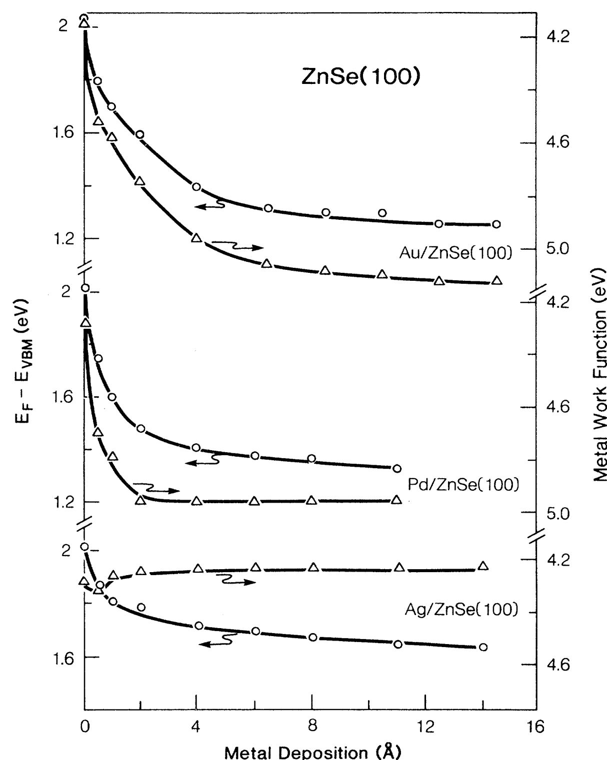

FIG. 7. Work function (right axis) and Fermi level position (left axis) for Au, Pd, and Ag deposition. For Au, the band bending and work function develop in a parallel way. The same correlation is observed for Pd, but to a lesser extent. For Ag, no correlation between work function and band bending is observed. The work-function scale was aligned so that in the Au case the initial work function and Fermi-level position coincide. Because of small deviations in the measured initial work function, the scales do not coincide. Note that the work function for high metal coverage is close to the work function of the bulk metal.

Finally, to gain additional insight into SBH formation, we correlated band bending and the development of the work function of the overlayer. We did this for Au, Ag, and Pd; the Au and Ag results are especially interesting because of the absence of surface disruption. The results

are summarized in Fig. 7. For Au, which formed a nondisruptive, layer-by-layer interface with ZnSe, band bending and work-function changes are parallel for coverages larger than ~2 Å. Deviations at lower coverage are caused by modifications of the surface dipole, as discussed extensively elsewhere.[35] For Pd, which disrupts the surface, work-function and band-bending changes behave in a similar way, but the agreement is less compelling than for Au. This may be because Pd disruption of the substrate continues to 10 Å or more Pd coverage, thus changing the interface dipole, or because the Pd work function is modified by surface segregation of Zn or Se. Although these surface-segregated atoms modify the work function, they have no influence on the buried metal-semiconductor interface. The results for Ag, which is also nondisruptive, show a behavior different from nondisruptive Au or disruptive Pd. From Fig. 7 the evolving SBH and work function show no resemblance at all. Indeed, the work function is almost constant (and close to the value of polycrystalline Ag film[32]) while E_F shifts gradually by ~0.4 eV. It is puzzling that the correlation between band bending and work function, that was so clear for Au, is absent for Ag. One may be tempted to attribute this discrepancy to the island-growth mode of Ag on ZnSe. The cutoff of the spectra may be caused by electrons originating from the exposed parts of ZnSe, and therefore would be typical for ZnSe rather than Ag. However, in that case both the Fermi-level position and work function should change by the same amount because the electron affinity of the semiconductor is independent of the Fermi-level position [Eq. (2)]. The fact that the cutoff does not shift to higher-binding energy proves that the electrons causing the cutoff originate from the Ag islands.

In conclusion, the alignment of the Fermi level at the metal-ZnSe interface cannot be described accurately by either the defect or MIGS models. The failure of the MIGS to completely pin the Fermi level in the case of ZnSe is not unexpected, because of the low dielectric constant of ZnSe.[6,30] There is a general correlation between the SBH and the metal work function for a wide range of metals, and the scatter can be accounted for by noting that the interface geometry is modified by chemistry and changes in effective electron affinity. For Au overlayers, there is a clear correlation between the evolving SBH and the metal work function, in agreement with the original Schottky model, but no such correlation was found for Ag, and there is less compelling correlation for Pd.

ACKNOWLEDGMENTS

This work was supported by the National Science Foundation (NSF) under Grant No. DMR 86-10837 and an IBM Materials Science and Processing Grant.

---

[1]L. J. Brillson, Surf. Sci. Rep. **2**, 123 (1982); J. H. Weaver, in *Analytical Techniques for Thin Films,* Treatise on Materials Science and Technology, edited by K. N. Tu and R. Rosenberg (Academic, New York, 1988), Vol. 27; W. E. Spicer, T. Kendelewicz, N. Newman, K. K. Chin, and I. Lindau, Surf. Sci. **168**, 240 (1986); R. Ludeke, *ibid.* **168**, 290 (1986).

[2]See, for example, K. Stiles, A. Kahn, D. G. Kilday, and G. Margaritondo, J. Vac. Sci. Technol. B **4**, 924 (1986); R. Cao, K. Miyano, T. Kendelewicz, K. K. Chin, I. Lindau, and W. E. Spicer, *ibid.* **5**, 998 (1987); K. Stiles and A. Kahn, Phys. Rev. Lett. **60**, 440 (1988).

[3]See, for example, C. F. Brucker and L. J. Brillson, Thin Solid Films **93**, 67 (1982) for CdSe and CdS interfaces; L. J. Brillson, C. F. Brucker, N. G. Stoffel, A. Katnani, R. Daniels, and G. Margaritondo, Physica B+C **117&118B**, 848 (1983); P. John, T. Miller, T. C. Hsieh, A. P. Shapiro, A. L. Wachs, and T.-C. Chiang, Phys. Rev. B **34**, 6704 (1986) for CdSe; M. Tang, D. W. Niles, I. Hernandez-Calderon, and H. Hochst, *ibid.* **36**, 3336 (1987) for Sn/CdTe; D. J. Friedman, I. Lindau, and W. E. Spicer, *ibid.* **37**, 731 (1988) for noble-metal–CdTe; and references therein.

[4]NBS Tables of Chemical Thermodynamic Properties, J. Phys Chem. Ref. Data **11**, Suppl. 2 (1982).

[5]S. Kurtin, T. C. McGill, and C. A. Mead, Phys. Rev. Lett. **22**, 1433 (1969).

[6]E. J. Mele and J. D. Joannopoulos, Phys. Rev. B **17**, 1528 (1978); S. G. Louie, J. R. Chelikowsky, and M. L. Cohen, *ibid.* **15**, 2154 (1977).

[7]A. B. McLean and R. H. Williams, J. Phys. C **21**, 783 (1988).

[8]J. R. Waldrop, J. Vac. Sci. Technol. B **2**, 445 (1984).

[9]W. E. Spicer, I. Lindau, P. R. Skeath, C. Y. Su, and P. W. Chye, Phys. Rev. Lett. **44**, 4 (1981).

[10]S. G. Anderson, F. Xu, M. Vos, J. H. Weaver, and H. Cheng, Phys. Rev. B **39**, 5079 (1989), for detailed analysis of the effects of interlayers for Au/Co/ZnSe and Co/Au/ZnSe interfaces.

[11]M. Vos, F. Xu, J. H. Weaver, and H. Cheng, Appl. Phys. Lett. **53**, 1530 (1988), discusses Schottky barrier control for Au/Al/ZnSe and Al/Au/ZnSe multilayers.

[12]J. M. DePuydt, H. Cheng, J. E. Potts, T. L. Smith, and S. K. Mohapatra, J. Appl. Phys. **62**, 4756 (1987).

[13]J. J. Joyce, M. del Giudice, and J. H. Weaver, J. Electron Spectrosc. Relat. Phenom. (to be published).

[14]C. E. Moore, *Atomic Energy Levels,* Nat. Bur. Stand. (U.S.) Circ. No. 467 (U.S. GPO, Washington, D.C., 1958).

[15]M. P. Seah and W. A. Dench, Surf. Interface Anal. **1**, 2 (1979).

[16]Effective mean-free paths for photoelectrons with ~10 eV relative to the Fermi level are shorter than predicted by the semi- empirical formula of Seah and Dench in Ref. 15 because of scattering of low-energy electrons associated with disorder and interface disruption. This has been discussed in detail by M. Vos, S. G. Anderson, and J. H. Weaver, Phys. Rev. B **39**, 3274 (1989). For the present results, we find that effective mean-free paths vary, being shortest for the most disruptive interfaces.

[17]W. A. Harrison, E. A. Kraut, J. R. Waldrop, and R. W. Grant, Phys. Rev. B **18**, 4402 (1978).

[18]T. Miller, E. Rosenwinkel, and T.-C. Chiang, Phys. Rev. B **30**, 570 (1984); J. A. Venables, J. Derrien, and A. P. Janssen, Surf. Sci. **95**, 411 (1980); K. Stiles, A. Kahn, D. Kilday, and G. Margaritondo, J. Vac. Sci. Technol. A **6**, 1511 (1988).

[19]See, for example, M. W. Ruckman, M. del Giudice, J. J. Joyce, and J. H. Weaver, Phys. Rev. B **34**, 5118 (1986) for Au/Ge; F. Xu, C. M. Aldao, I. M. Vitomirov, and J. H. Weaver, Appl. Phys. Lett. **51**, 1946 (1987) for Au/Si; F. Xu, Y. Shapira, D. M. Hill, and J. H. Weaver, Phys. Rev. B **35**, 7417 (1987) for Au/GaAs; Y. Shapira, L. Brillson, A. D. Katnani, and G. Margaritondo, Phys. Rev. B **30**, 4856 (1984) for Au/InP; Y. Shapira, F. Boscherini, C. Cappasso, F. Xu, D. M. Hill, and J. H. Weaver, Phys. Rev. B **36**, 7656 (1987) for Au/InSb, and extensive literature cited therein.

[20]J. H. Weaver, Z. Lin, and F. Xu, in *Surface Segregation and Related Phenomena,* edited by P. A. Dowben and A. Miller (CRC, Boca Raton, in press). A shorter version can be found in Z. Lin, F. Xu, and J. H. Weaver, Phys. Rev. B **36**, 5777 (1987).

[21]F. J. Himpsel, D. E. Eastman, E. E. Koch, and A. R. Williams, Phys. Rev. B **22**, 4604 (1980).

[22]N. G. Stoffel, M. Turowski, and G. Margaritondo, Phys. Rev. B **30**, 3294 (1984); T. Kendelewicz, M. D. Williams, W. G. Petro, I. Lindau, and W. E. Spicer, Phys. Rev. B **31**, 6503 (1985).

[23]A. R. Miedema, P. F. de Châtel, and F. R. de Boer, Physica B+C **100B**, 1 (1980).

[24]B. Johansson and N. Mårtensson, Phys. Rev. B **21**, 4427 (1980).

[25]M. Cardona and L. Ley, in *Photoemission from Solids* (Springer-Verlag, Berlin, 1978).

[26]S. M. Sze, *Physics of Semiconductor Devices,* 2nd ed. (Wiley, New York, 1981).

[27]W. Schottky, Z. Phys. **113**, 367 (1939).

[28]J. Bardeen, Phys. Rev. **71**, 717 (1947).

[29]I. Lindau and T. Kendelewicz, CRC Crit. Rev. Solid State Mater. Sci. **13**, 27 (1987).

[30]C. Tejedor and F. Flores, J. Phys. C **12**, 731 (1979); J. Tersoff, Phys. Rev. Lett. **52**, 465 (1984).

[31]M. Cardona and N. E. Christensen, Phys. Rev. B **35**, 6182 (1987).

[32]H. B. Michaelson, J. Appl. Phys. **48**, 4729 (1977).

[33]A. B. McLean and R. H. Williams, J. Phys. C **21**, 783 (1988).

[34]R. E. Viturro, J. L. Shaw, C. Mailhiot, L. J. Brillson, N. Tache, J. Mckinley, G. Margaritondo, J. M. Woodall, P. D. Kirchner, G. D. Pettit, and S. L. Wright, Appl. Phys. Lett. **52**, 2052 (1988).

[35]F. Xu, M. Vos, J. H. Weaver, and H. Cheng, Phys. Rev. B **38**, 13 418 (1988).